

Bond-disordered Anderson model on a two dimensional square lattice — chiral symmetry and restoration of one-parameter scaling

Viktor Z. Cerovski

Department of Physics and Astronomy, Michigan State University, East Lansing, MI 48824

(Submitted to PRB on January 27, 2000.)

Bond-disordered Anderson model in two dimensions on a square lattice is studied numerically near the band center by calculating density of states (DoS), multifractal properties of eigenstates and the localization length. DoS divergence at the band center is studied and compared with Gade's result [Nucl. Phys. B **398**, 499 (1993)] and the powerlaw. Although Gade's form describes accurately DoS of finite size systems near the band-center, it fails to describe the calculated part of DoS of the infinite system, and a new expression is proposed. Study of the level spacing distributions reveals that the state closest to the band center and the next one have different level spacing distribution than the pairs of states away from the band center. Multifractal properties of finite systems furthermore show that scaling of eigenstates changes discontinuously near the band center. This unusual behavior suggests the existence of a new divergent length scale, whose existence is explained as the finite size manifestation of the band center critical point of the infinite system, and the critical exponent of the correlation length is calculated by a finite size scaling. Furthermore, study of scaling of Lyapunov exponents of transfer matrices of long stripes indicates that for a long stripe of any width there is an energy region around band center within which the Lyapunov exponents cannot be described by one-parameter scaling. This region, however, vanishes in the limit of the infinite square lattice when one-parameter scaling is restored, and the scaling exponent calculated, in agreement with the result of the finite size scaling analysis.

PACS numbers: 71.23.An, 72.15.Rn, 73.20.Fz

I. INTRODUCTION

A quantum particle moving in a random potential undergoes Anderson localization quantum phase transition in three dimensions with increasing of the strength of disorder [1–4]. The order parameter characterizing the localized phase is the inverse localization length ξ^{-1} [5], describing the exponential decay of the envelope of eigenstates. When the critical point is being approached from the localized phase, localization length, which depends for a given energy only on the strength of the disorder, increases with decreasing of the disorder strength and finally diverges as a power-law at a particular disorder strength. Further decrease of disorder strength then makes the eigenstate extended throughout the whole system. Simultaneously, on length scales smaller than the localization length, eigenstates

exhibit multifractal scaling behavior characterized by anomalous scaling of the inverse participation numbers (for definitions and references, see Sec. V).

This basic phenomena, together with the work of Thouless on the scaling of conductance in finite-size systems [6], led to the scaling theory of localization [7,8], one of the main consequences of which is the absence of extended states in two dimensional disordered systems, with two dimensions being the lower critical dimension of the transition. If the spin-orbit interaction is present, however, picture changes and two dimensional systems from symplectic ensemble exhibit localization transition even in two dimensions as opposed to systems from orthogonal ensemble which have all states localized [3]. Presence of the strong magnetic field in two dimensional disordered systems, on the other hand, leads to a completely different behavior – the integer quantum Hall effect (IQHE) – where critical states are present at the middle of each of disorder-broadened Landau levels [9].

Another class of models exhibiting localization properties different from the systems mentioned above are systems with chiral (particle-hole) symmetry. Such systems are defined on a bipartite lattice with only hopping (off-diagonal or bond-) disorder. Wegner was first to realize the importance of this symmetry in disordered systems [13–15], and even one-dimensional systems with this symmetry are known to have peculiar properties, such as diverging DoS at the band center [10], where the eigenstate decays as $\exp(-\gamma\sqrt{r})$ [11,12], in contrast to one-dimensional site-disordered systems which have DoS bounded [16] and all states localized.

There are several models with chiral symmetry that have been extensively studied. The simplest two, in the sense that only one orbital per site and nearest neighbor hopping are included, time-reversal symmetry present and the spin not relevant, are the Anderson bond-disordered model (ABD) [10–12,19,20] and the random Dirac fermion model (RDF) [17,18]. The main difference between these two models is that, in the non-disordered case, ABD model has a line of points as the Fermi surface at half-filling while RDF has a point Fermi surface and linear dispersion of energies.

This work is concerned with the ABD model on a square lattice of size L and periodic boundary conditions, defined by the Hamiltonian:

$$H = -\epsilon_0 \sum_{\langle i,j \rangle} (t_{i,j} c_i^\dagger c_j + \text{H.c.}), \quad (1)$$

where brackets denote neighboring sites on the lattice, c_i is annihilation operator of the electron at site i , and t 's are uniformly distributed random variables $t_{i,j} \in (1 - 2w, 1)$, with $0 < w \leq 1$. They represent random hopping energies between nearest neighbors, expressed in units of energy ϵ_0 , which is set to 1 hereafter.

Interest in this model mainly comes from its unusual scaling properties at the band center, where Soukoulis *et. al* [19] have found critical state at the band center using Green's function [8] and transfer matrix method (TMM) [22]. More recent TMM calculation by Eilmes *et. al* [20] confirmed this result with a higher accuracy and showed the validity of one-parameter scaling not too close to the band center. Nevertheless, Miler and Wang [21] have found in their study of two models with chiral symmetry an apparent band of extended states near the band center, and it remained unclear what is the fate of these states in the infinite 2D system. Another study [23] yet showed that scaling exponent of the average participation number changed discontinuously near the band center, and the explicit dependence of this

energy on the system size proposed by authors implied the existence of another diverging length scale in the problem. The last effect is rather subtle to calculate and led to a different participation number scaling exponent of the ABD model at the band center in Ref. [20] compared to the one calculated here, as discussed in detail in Sec. V below. Furthermore, Brouwer *et al.* [24] have calculated conductance distribution of quantum wires described by (1), and showed its non-universality and necessity to introduce an additional microscopic parameter.

It is thus goal of this paper to present a detailed study of the scaling of localization length on the approach to the band center for an infinite 2D square lattice, and test the validity of one-parameter scaling, as well as to calculate the multifractal properties of the electron probability density on length scales smaller than the localization length. Also a new analytical expression for the DoS of the infinite two-dimensional system near the band center is proposed. This paper is organized as follows: Some general properties and exact results are presented in Sec. II; Calculation of DoS is presented and analyzed in Sec. III; Sec. IV contains analysis of level spacing distributions between the nearest neighbors; Multifractal properties of eigenstates are studied in Sec. V; Scaling of the Lyapunov exponents of transfer matrices of long strips and the scaling of localization length are studied in Sec. VI; and, finally, Sec. VII summarizes results of this work.

II. SOME GENERAL PROPERTIES OF LATTICE HAMILTONIANS WITH CHIRAL SYMMETRY

Suppose that the lattice is composed of two sublattices A and B with, respectively, N_A and N_B sites. The corresponding bond-disordered Hamiltonian with chiral symmetry then has the form:

$$H = \sum_{i \in A, j \in B} (t_{i,j} c_i^\dagger c_j + \text{H.c.}), \quad (2)$$

It is easy to show that for every eigenstate $|\psi\rangle$ with energy E there is an eigenstate with energy $-E$ with a wavefunction that has the opposite sign at each site of one of the two sublattices.

If the total number of sites $N = N_A + N_B$ is odd and open boundaries condition is applied (in order to keep the symmetry), then, since all eigenstates come in the opposite energy pairs, there will be exactly one state with eigenenergy 0. This can be furthermore generalized, and if $m = N_A - N_B > 0$, there exist exactly m zero-energy eigenstates that have vanishing amplitude on the sublattice B [15,25].

On the other hand, if $m = 0$, the electron has equal probability of occupying each of the two sublattices. To show this, (2) is represented in the basis where the first and second half of basis vectors are eigenstates of the position operator on sites of sublattice A and B , respectively. The Hamiltonian is then represented as

$$H = \begin{pmatrix} 0 & M \\ M^\dagger & 0 \end{pmatrix}, \quad (3)$$

where M is a square matrix of hopping elements from one sublattice to the other. Eigenstate $|\psi\rangle = \begin{pmatrix} |\psi_A\rangle \\ |\psi_B\rangle \end{pmatrix}$ satisfies:

$$E = \langle \psi | H | \psi \rangle = 2 \operatorname{Re} \langle \psi_A | M | \psi_B \rangle. \quad (4)$$

On the other hand,

$$H | \psi \rangle = \begin{pmatrix} M | \psi_B \rangle \\ M^\dagger | \psi_A \rangle \end{pmatrix} = \begin{pmatrix} E | \psi_A \rangle \\ E | \psi_B \rangle \end{pmatrix}. \quad (5)$$

From (4) and (5) now follows that, for ABD model, $\langle \psi_A | \psi_A \rangle = 1/2$.

In this work only even L finite size systems on a square lattice with periodic boundary conditions are studied, because one of the main goals of this work is to understand the vicinity of the critical point of ABD model on the infinite square lattice, which in turn has $m = 0$, while the limit $L \rightarrow \infty$ for odd L and open boundary conditions has $m = 1$.

III. DENSITY OF STATES NEAR THE BAND CENTER

Density of states (DoS) is calculated by exact numerical diagonalization of finite size Hamiltonians for various L for many configurations of disorder, and binning of eigenenergies. Obtained DoS for each system size, $\rho_L(E)$, are normalized to 1. The L dependent parts of such obtained $\rho_L(E)$ are then removed leaving L independent DoS $\rho(E)$, which is therefore expected to be correct in the $L \rightarrow \infty$ limit. The removal of finite size dependency is based on an observation that DoS converges quickly away from the band center with increasing of L . Thus, only a small number of eigenenergies (up to 20) closest to the band center and corresponding DoS histograms has been calculated for each L . The calculated $\rho_L(E)$ plotted on a single graph revealed that three bins closest to the band center are where the system size dependence sets in. Their removal thus led to the DoS $\rho(E)$ of the infinite system.

Results for $\rho_L(|E|)$ are given in Fig. 1, for system sizes $L = 10, 20, \dots, 60$ and number of disordered configurations ranging, respectively, from 160000 to 4100. They are fitted to a powerlaw divergence $\rho_L(E) = C_L |E|^{-\alpha_L}$, as well as to the Gade's result [14]:

$$\rho_L(E) = C_L \frac{1}{|E|} \exp \left(-\kappa_L \sqrt{-\ln |E|} \right). \quad (6)$$

All the calculations were done for several different number of bins, and the obtained values of fitting parameters were the same within error bars.

The figure 1 shows that (6) describes ρ_L very accurately for $L \geq 40$, including the size-dependent part. The powerlaw, on the other hand, also describes the data accurately for same system sizes, but fails to describe the L -dependent part of ρ_L . Despite this, neither of the two forms describe the whole $\rho(E)$ accurately. Instead, the expression found to best fit the obtained L -independent DoS, given in Fig. 2, is

$$\rho(E) = C \frac{1}{\sqrt{|E|}} \exp \left(-\kappa \sqrt{-\ln |E|} \right), \quad (7)$$

with $\kappa = 1.345 \pm 0.005$ and $C = 1.30 \pm 0.03$, represented by the full line in the same figure. The observed range in which (7) is accurate is for all the energies studied smaller than 6×10^{-2} .

IV. DISTRIBUTION OF THE NEAREST-NEIGHBOR LEVEL SPACINGS

In the localized regime, an eigenstate is determined mainly by a local configuration of disorder where the wavefunction is localized, and two eigenstates close in energy are spatially far apart. Level repulsion is therefore absent and the distribution of the nearest neighbor level spacings $s \equiv E_{i+1} - E_i$ is Poissonian [26],

$$D_P(s) = \frac{1}{\delta} \exp\left(-\frac{s}{\delta}\right). \quad (8)$$

where $\delta \equiv \langle s \rangle$ is the mean level spacing.

In the delocalized phase, on the other hand, eigenstates are extended throughout the system and level repulsion becomes significant for eigenstates with close energies. In the infinite 3D Anderson site-disordered model (ASD),

$$H = \sum_i \epsilon_i n_i - \sum_{\langle i,j \rangle} (c_i^\dagger c_j + c_j^\dagger c_i), \quad (9)$$

with uniformly distributed $\epsilon_i \in (-W/2, W/2)$, distribution of level spacings becomes that of Gaussian orthogonal ensemble (GOE) [26], very accurately described by the Wigner surmise

$$D_W(s) = \frac{\pi}{2} \frac{s}{\delta^2} \exp\left(-\frac{\pi}{4} \left(\frac{s}{\delta}\right)^2\right). \quad (10)$$

In finite-size systems, localized states are on average at a distance L rather than infinitely far apart. This leads to a repulsion between adjacent energy levels and non-universal distribution $D_L(s)$. Shklovskii *et. al.* [26] have shown that $D_L(s)$ of the 3D site-disordered Anderson model exhibits linear dependence on s characteristic for $D_W(s)$ for small s and exponential tail characteristic for $D_P(s)$ for large s . They were able, from the finite size scaling analysis of the tail, to accurately determine the critical point and exponent. In the infinite size limit, they have recovered not only $D_P(s)$ in the insulating phase and $D_W(s)$ in the conducting phase, but also a system size independent non-universal distribution at the critical point which was furthermore shown by Braun *et. al.* [27] to be dependent on boundary conditions. This method was also used for an accurate determination of localization length in two dimensional ASD model [28], confirming the absence of delocalized states following the scenario of the insulating phase from Ref. [26] described above.

To see the effect of symmetry of the Hamiltonian (2) on the distribution of level spacings, let us for a moment consider i -th eigenenergy E_i of the ASD model. Upon averaging over disorder, the E_i will be distributed between E_i^{min} and E_i^{max} according to some distribution. Some of the eigenenergies, for i close to $N/2$, will have $E_i^{min} < 0 < E_i^{max}$. This is, however, forbidden for eigenstates of the ASD model since every E_i of (2) is negative for $i < N/2$ and positive for $i > N/2$. This means that eigenenergies of (2) close to the band center are effectively pushed away from it due to the symmetry. If L is much smaller than the localization length, states will be repelled among themselves due to their large spatial overlap. But the two states closest to the band center, being simply related to each another by the symmetry, will not repel at all, *i.e.* the state closest to the band center is at the (high energy) end of the spectrum. Thus, these two states are distributed around zero, where distributions of all other individual levels go to zero.

To explore consequences of this simple analysis, the level spacing distribution is calculated between each pair of adjacent levels separately. Let us denote by $D_i(s)$ level spacing distribution between i and $i+1$ energy level after unfolding of spectrum [29], *i.e.* expressing level energies in units of mean level spacing, where $0 < E_1 < E_2 < \dots < E_{N/2}$. Figure 3 shows $D_1(s), \dots, D_5(s)$, for $L = 20, 40$ and, respectively 150000, 120000 configurations, and it can be seen that $D_1(s)$ is distinctly different than $D_2(s), \dots, D_5(s)$. The same effect was also present for $L = 10, 30$, while for $L = 50$ and 60 the number of disorder configurations was insufficient for accurate enough determination of individual $D_i(s)$ [30]. This illustrates how the presence of chiral symmetry can profoundly influence spectral characteristics near the band center, despite the fact that DoS of ABD and ASD models seem to have same shape for adequately chosen pairs of disorder parameters w and W away from the band center (and after rescaling of ϵ_0) [20].

V. MULTIFRACTALITY OF EIGENSTATES

Eigenstate of an electron in the random potential fluctuates from site to site and it was proposed that the eigenstate at the mobility edge in disordered systems in general should have fractal structure [31], and shown that even localized states in one and two dimensions exhibit fractal character on length scales smaller than the localization length [32,33].

Inverse participation numbers Z_q (IPN) are particularly convenient quantities to describe scaling properties of probability distribution of the electron. IPN of an eigenstate Ψ are defined as:

$$Z_q(\Psi) \equiv \sum_{i=1}^{L \times L} |\Psi(\mathbf{r}_i)|^{2q}. \quad (11)$$

Intuitively, their meaning can be seen by looking at the participation number $Z_2(\Psi)^{-1}$: it is equal to 1 for a state localized at one site and to N for plane-waves. Participation number thus gives generally the number of sites at which the wavefunction is significantly different than zero. Participation numbers $Z_q(\Psi)^{-1}$ then generalize this by giving the number of sites where probability distribution of electron is very high (for large positive q 's), very low (for large negative q 's), and in between these extrema, continuously parameterized by q .

More convenient, with the advantage of being defined as averages over disorder at a given energy E , are IPN defined as functions of E and system size L ,

$$Z_q(L, E) \equiv \langle Z_q(\Psi) \delta(E(\Psi) - E) \rangle, \quad (12)$$

where the brackets denote averaging over disorder. $Z_q(E, L)$ can be numerically calculated by averaging (11) over all eigenstates from M configurations of disorder belonging to an energy interval of width ΔE around E , and studying the limit $\Delta E \rightarrow 0$ for large M [23].

Wegner [34] pioneered this kind of investigations, and Castellani and Peliti [35] proposed that eigenstates near the critical point are multifractal on length scales smaller than ξ . The most important feature of IPN of eigenstates is their scaling with system size and energy [34,35]:

$$Z_q(L, E) \sim L^{-\tau_q}, \quad (13)$$

$$Z_q(L, E) \sim |E - E_c|^{\pi_q}, \quad (14)$$

where E_c is the critical energy. The former scaling is present at any E for $L \ll \xi(E)$, while the latter holds in the critical region of the transition [39].

Within the framework of multifractality [36,37], electron probability density is characterized by several quantities that can be derived from τ_q — the generalized dimension D_q and the singularity strength α_q of the q -th singularity with the fractal dimension f_q :

$$(q - 1)D_q \equiv \tau_q, \quad \alpha_q \equiv \frac{d\tau_q}{dq}, \quad f_q(\alpha_q) \equiv \alpha_q q - \tau_q. \quad (15)$$

D_q represents generalization of the fractal dimension, and it is constant and equal to the fractal dimension for ordinary fractals, while $f_q(\alpha_q)$ is the singularity strength spectrum describing multifractal as an interlaced set of fractals with fractal dimensions f_q , where the measure on the q -th fractal scales as a powerlaw with exponent α_q . These quantities have several general properties: D_0 is the fractal dimension of the support (two in this work); D_1 is called information dimension since it describes scaling of the entropy of the measure [38], and there exist finite $D_{min} = D_{q \rightarrow \infty}$ and $D_{max} = D_{q \rightarrow -\infty}$.

This work is concerned mainly with the spectrum of generalized dimensions D_q characterizing the spatial structure of eigenstates on the length scales smaller than the localization length, while the properties of π_q will be discussed elsewhere. Before detailed discussion of the results, an overview of the main results of this part of the paper is given. Scaling of IPN at the band center is calculated first, and shown that scaling properties (that is, whole spectrum of generalized dimensions D_q) changes discontinuously near the band center, at an energy $E'(L)$ for a range of L studied. It is then shown that E' can be quite accurately identified with the half of the width of the energy range around band center within which two states occur on average in the ensemble of disordered systems. Existence of this energy reveals the existence of a length scale $\xi'(E)$, diverging when $E \rightarrow 0$, that is the system size at which IPN change their scaling properties from one powerlaw dependence on L to another. This change is then explained as a finite size manifestation of the critical point, and the critical exponent calculated by a finite-size analysis.

Calculation of $Z_q(E, L)$ starts with calculation of $Z_q(E, L, \Delta E)$, which is just IPN averaged over all eigenstates from an energy interval $(E - \Delta E/2, E + \Delta E/2)$, taken from N_Ω realizations of disorder, followed by studying the limit $\Delta E \rightarrow 0$ [23]. Results at the band center for system $L = 80$ and several different q 's, are presented in Fig. 4. The error bars in the figure are taken to be the standard deviation of average value.

The figure suggests the existence of an energy E' independent of q (and therefore defined by the whole multifractal measure) such that decreasing ΔE below E' does not change $Z_q(E, L, \Delta E)$ significantly. Decreasing of Z_q to a smaller extend, however, is still present for $\Delta E < E'$, and the main source of this is the mismatch between average and typical value of IPN at a given energy. Thus, the effect should become smaller as the number of disorder configurations that are averaged over is increased, and $Z_q(E, L, \Delta E < E') \approx Z_q(E, L)$ up to the corresponding statistical error. This can be seen in Fig. 4 and 5, where values of Z_q for $\Delta E < E'$ are approximately constant within the error bars (as indicated by the horizontal dashed lines), while for $\Delta E > E'$ there is approximately linear dependence of Z_q on the bin size ΔE . In this sense Figure 5 suggests that E' exists for all the systems studied (and can be shown to be independent of q for each of them analogously as shown in Fig. 5).

Analogous analysis is carried out for energies away from the band center and $Z_q(E, L)$ determined accordingly, where it turns out that the convergence for these energies is slightly

easier to establish and occurs at larger ΔE than at the band center. Such obtained energy intervals used in calculations of IPN for different E were small enough so that there was practically no overlap among them.

The vertical dashed lines in Fig. 4 and Fig. 5 represent half of the energy $E_2(L)$, defined as the width of the energy interval around zero in which every system from the ensemble of disordered systems has two states on average [23],

$$1 = L^2 \int_{E_2/2}^0 \rho_L(\epsilon) d\epsilon. \quad (16)$$

From the figures one can see that $E' \approx E_2/2$ for all system sizes studied except $L = 40$ (the smallest system studied, not shown in Fig. 5), where the convergence seems to be somewhat slower. Equation (16) defines a new length scale $\xi'(E)$ that can be described as the system size L for a given energy E such that the number of states within the energy interval between $-E$ and E is two on average. This can be defined as

$$\xi'(E) = E_2^{-1}(E), \quad (17)$$

where $E_2^{-1}(E)$ is the inverse function of the $E_2(L)$, which is defined by (16). Since $E_2(L)$ goes to zero when $L \rightarrow \infty$, the new length scale diverges when $E \rightarrow 0$.

It is tempting to integrate results for ρ_L from Sec. III to obtain $\xi'(E)$ explicitly. This, however, does not give the correct result since the whole analysis of DoS from Sec. III is done for energies larger than the width of the distribution of two states closest to the band center, which in turn defines ξ' in (17). In other words, there is an energy cutoff, vanishing when $L \rightarrow \infty$, below which the fits are not accurate, most obviously seen by noticing that all of the assumed analytical forms of ρ_L are diverging at the band center, while the actual ρ_L is not.

Nontrivial feature connected with the existence of the new length scale ξ' is that scaling exponents $\tau_q(E)$ are different for $L \lesssim \xi'(E)$ and $L \gtrsim \xi'(E)$. This is a generalization of findings from Ref. [23], where a deviation from the powerlaw scaling of the average participation number for different ΔE at the band center appeared whenever ΔE exceeded $E'(L)$ in several models with chiral symmetry. It can be straightforwardly shown that same happens with scaling of $Z_q(E = 0, L, \Delta E)$. This suggests that a new scaling characteristic should be attributed to the two states closest to the band center, and that E' scales as E_2 , with a coefficient of proportionality close to one. This also implies that the corrections to the constant $Z_q(E, L, \Delta E)$ for $\Delta E < E'$ are small. Therefore, the length at which change of scaling occurs should be close to and depend on the energy proportionally to $\xi'(E)$, while the change of scaling should be a narrow crossover, as opposed to much broader crossover from powerlaw to constant IPN that occurs at the termination of multifractal scaling (13) for $L \approx \xi$.

This is compatible with the results presented in Fig. 6, which gives calculated $Z_q(L, E)$, for $q = 0.9, 2$ as well as for all L and E studied. Smaller q 's allow for more accurate determination of the scaling properties, and it can be seen from the data that for both q 's there are two characteristic scaling behaviors — one occurs at the band center and nearby energies for smaller L , while the other scaling holds at energies further away from the band center, and for larger L at energies close to the band center.

Scaling exponents τ_q are determined from the linear regression of the data for system sizes $L = 50, 60, \dots, 100$. Goodness of the powerlaw fit is quantitatively characterized by a coefficient $\gamma_q(E)$ next to the quadratic term from an additional quadratic fit of the data. Such obtained τ_q and γ_q from the data in Fig. 6 are presented in Fig. 7. Results show the existence of three different cases: (i) away from the band center, $\gamma_q \approx 0$ and τ_q is independent of E , indicating powerlaw dependence of IPN on L ; (ii) approaching the band center, γ_q becomes different than zero, indicating that powerlaw is not obeyed. This is due to the emergence of the new scaling for system sizes $L \gtrsim \xi'(E)$ discussed above and present in Fig. 6; and (iii) for $E = 0$ powerlaw is obeyed again ($\gamma_q \approx 0$), but with a different τ_q than for energies away from the band center.

Discontinuity of $\tau_q(E)$ for all the other q 's studied naturally leads to two different spectra of generalized dimensions, and Fig. 8 shows calculated D_q for all energies except the three nonzero energies closest to the band center (which cannot give τ_q from the fitting procedure used here due to the change of scaling properties discussed above). In particular, the participation number grows with the number of sites L^2 as a powerlaw with exponents $\beta(E = 0) = 0.25 \pm 0.02$, and $\beta(E \neq 0) = 0.55 \pm 0.05$. This should be compared with the result for ABD model of Ref. [20], $\beta(E = 0) = 0.50 \pm 0.06$. It is easy to explain this discrepancy since the bin size $\Delta E = 4 \times 10^{-4}$ used in Ref. [20] was, depending on the system size, roughly over an order of magnitude too large to detect the correct scaling behavior, and therefore $\beta(E \neq 0)$ was obtained instead.

D_q is calculated for only three negative values of q , mainly because IPN for negative q 's are determined mostly by the parts of eigenstates with the smallest probability to find the electron, which in turn acquire the highest relative error during numerical diagonalization of the Hamiltonian. Difficulties in calculating D_q in this regime even arose suspicion that multifractality might break down for negative q [40]. It is thus important to show that D_q is defined for negative q 's as well as for positive ones. Accuracy of all the calculations of IPN done in this section can be straightforwardly improved by increasing the number of configurations of disorder that was averaged over. This would lead to smaller error bars of all the quantities calculated, as well as to the wider range of q 's for which D_q can be calculated.

Results of this section give the following picture of the scaling of IPN with system size: for any energy E close enough to the band center, there exist two powerlaw scalings: one for $L_0 < L \lesssim \xi'(E)$ described by the set of exponents $\tau_q(E = 0)$, and another one for $\xi'(E) \lesssim L \ll \xi(E)$, described by a *different* set of exponents $\tau_q(E \neq 0)$, which leads to the two different spectra of generalized dimensions D_q .

Dependence of the new length scale on energy, $\xi'(E)$, can be easily determined from (17) by integrating the actual numerical data for $\rho_L(E)$, and the result, obtained from Fig. 9, gives $\xi'(E) \propto |E|^{-\nu'}$, with

$$\nu' = 0.35 \pm 0.01 . \quad (18)$$

The meaning of this new length scale and corresponding exponent ν' can be understood by assuming that the additional scaling of the two states is due to the finite size effect of “smearing” of the $E = 0$ critical point of the infinite system, because exactly the two states closest to the band center become critical when $L \rightarrow \infty$. The critical energy then changes by $\Delta\epsilon$ which is, in a finite system of size L (in units of the lattice spacing), equal

to $\Delta E_2(L) \propto L^{-\delta} = L^{-1/\nu'}$. If furthermore $\xi \propto |E|^{-\nu}$ in the infinite system, the shift $\Delta\epsilon_c$ of the critical energy in the system of size L is $\Delta\epsilon_c \propto L^{-1/\nu}$, from the general theory of the finite size scaling [41]. Therefore, ν' equals ν , the critical exponent of the correlation length of the infinite two-dimensional system. It should be noticed that the finite size scaling applied here is somewhat different than usual, where $\Delta\epsilon_c \equiv |E - E_c|/E_c$ [41]. Here, $E_c = 0$ and $\Delta\epsilon_c \equiv |E - E_c|$, where both energies are expressed in units of ϵ_0 , as discussed in the Introduction. Thus, energy ϵ_0 appears in the denominator of $\Delta\epsilon_c$ rather than the critical energy itself.

VI. LOCALIZATION LENGTH NEAR THE BAND CENTER

In order to calculate the localization length of the infinite two dimensional system, finite-size scaling analysis of MacKinnon and Kramer [8] (FSS) is applied to TMM of Pichard and Sarma [22]. In this analysis, inverse Lyapunov exponents (ILE) of the transfer matrix of the ABD model [20,24] of a long quasi one dimensional strip of width M are calculated for several energies near the band center and one parameter scaling analysis applied to the largest ILE, from which the correlation length of 2D system is calculated. The scaling analysis consists of assuming that the change of the largest ILE, $\Lambda(E, M)$, due to rescaling $M \rightarrow bM$ can be compensated by an appropriate change of energy, after which Λ will remain the same, which implies that [8]

$$\Lambda(E, M) = \Lambda(M/\xi(E)). \quad (19)$$

Figure 10 shows the calculated $\Lambda(E, M)$ for several energies E close to the band center and for various strips up to 128 sites wide. The figure also gives the second largest (dashed line) renormalized ILE, Λ_2 , for the two lowest non-zero energies studied ($E = 10^{-5}$ and 10^{-6}) and for $M \leq 20$. All values are obtained with relative error of 1% or better.

At $E = 0$ and for M even, all ILE become doubly degenerate due to the presence of chiral symmetry [21,24], and they scale linearly with M for $M \geq 16$, reflecting the scale invariance of Λ characteristic of a critical state. To see the effect this degeneracy has on scaling properties of ILE, we should recall that ILE of transfer matrices of disordered systems repel each other in general [42] and become self-averaging quantities for sufficiently long stripes [22]. The symmetry now enforces “dimerization” of pairs of ILE, acting as an effective attractive force between each pair of ILE that become degenerate at zero energy, as in Fig. 10, where, for a fixed M , Λ and Λ_2 are closer together for the smaller energy. The largest ILE thus decreases in a strip of width M on approaching the band center, as in models with chiral symmetry studied in Ref. [21]. On the other hand, at any given energy, every pair of ILE becomes more repelling with increasing of M . Such increased number of ILE thus diminishes the attractive effect of the symmetry, and, depending on the relative strengths of the two effects, there are two regimes: (i) for smaller M , the largest ILE increases approximately linearly with M , and, since the slope of the rise changes with energy, FSS cannot be done; (ii) for sufficiently large M , on the other hand, the repulsion among ILE due to disorder dominates and FSS is possible.

The one-parameter universal function $\Lambda(M/\xi(E))$, obtained for system sizes $M \geq 50$ for energies $|E| > 10^{-4}$, and for system sizes $M \geq 64$ for energies $10^{-5} \leq |E| \leq 10^{-4}$, is

presented in Fig. 11. The obtained localization length $\xi(E)$, in units of the localization length of the smallest energy studied ($E = 0.1$), is shown in the inset of the same figure. Calculated $\xi(E)/\xi(0.1)$ is fitted to the powerlaw for energies $10^{-5} \leq E \leq 10^{-3}$, and the result suggests powerlaw diverging localization length at the band center, with the exponent

$$\nu = 0.335 \pm 0.034, \quad (20)$$

in agreement with the result (18) of Sec. V.

In Ref. [20], the authors also calculated one-parameter scaling curves for energies further away from the band center than in this work and found that there is a universal curve for a large set of ABD systems with different w that they studied. The obtained one-parameter function suggested that $\Lambda(x)$ either grows indefinitely when $E \rightarrow 0$, which is similar to the two dimensional ASD model [8] or becomes constant. If this result were correct, however, for the smaller energies than studied there, it would imply that localization length at the band center either diverges logarithmically, as in the 2D ASD model, or that it has a finite limiting value. We see therefore that, although correct in the energy range studied in Ref. [20], the picture of a single scaling curve for different w from the same work should break down for smaller energies, since the powerlaw diverging ξ requires that $d \ln \Lambda / d \ln M$ goes to zero when $E \rightarrow 0$, and separate one-parameter scaling curves exist for each w .

Some additional analysis of the results can be done by introducing $\Lambda_{max}(M)$, defined as the maximal $\Lambda(E, M)$ for a given strip width M . Importance of this quantity comes from the fact that points where Λ reaches its maximum for various energies cannot be described by FSS, and, at the same time, Λ_{max} limits by its definition possible values that $\Lambda(x)$ (obtained from the FSS) can have. The main observation is that Λ_{max} seems to grow slower than linearly in Fig. 10. Linear (or faster) growth would imply existence of an additional energy scale below which FSS would break down for all large M and $\Lambda(E, M)$ would grow linearly and indefinitely with M in the same figure, implying the existence of a whole band of extended states where one-parameter scaling would not hold. Slower than linear growth of Λ_{max} seen, therefore, furthermore suggests the existence of a single critical point at the band center of the system on an infinite square lattice.

VII. CONCLUSIONS

In conclusions, main results of this work are summarized. Density of states of finite size systems are calculated and shown the validity of Gade's expression (6). The calculated part of the DoS for the system on an infinite square lattice, however, suggests a different dependence on energy near the band center,

$$\rho(E) = C \frac{1}{\sqrt{|E|}} \exp\left(-\kappa \sqrt{-\ln |E|}\right), \quad (21)$$

with $\kappa = 1.345 \pm 0.005$ and $C = 1.30 \pm 0.03$.

Other calculated quantities share in common a qualitative feature of a discontinuous change near or at the band center. The nearest neighbor level spacing distributions, for instance, between the state closest to the band center and the next one seem to be distinctly different than the level spacing distributions between other neighboring states. This was

argued to be connected to the chiral symmetry of the model, which places the two states closest to $E = 0$ at the (high energy) end of the spectrum. These two states are furthermore found to play a crucial role in explaining the discontinuous change of the scaling properties of IPN near the band center. Extrapolation to the limit of infinite square lattice then led to the two different spectra of generalized dimensions D_q — one for $E \neq 0$ (present at the length scales smaller than the localization length), and another one for $E = 0$ (present at all length scales). Finite size scaling associated with the effects that finite L has on the critical band center states of the infinite system led to the value $\nu = 0.35 \pm 0.01$ of the critical exponent of the localization length.

Additional scaling analysis of ILE of transfer matrices of long quasi-1D systems gave the value $\nu = 0.335 \pm 0.034$. This suggests that there is only one critical state at the band center with all other states localized in the system on the infinite square lattice, in agreement with findings of Ref. [32,20]. One parameter universal function $\Lambda(x)$ is calculated and another discontinuity found, since $\Lambda(x(E \rightarrow 0)) \neq \Lambda(E = 0, M)$.

A puzzling feature of the critical exponent ν of the ABD as well as of the RDF model [17,18] is their apparent disagreement with the rigorous theorem of Chayes and Chayes *et al* [43], which states that $\nu \geq 1$ in two-dimensional quantum disordered systems in general. This question, however, requires further study and will be addressed elsewhere.

ACKNOWLEDGMENTS

This work is partially supported by the Department of Physics and Astronomy at Michigan State University. Author is thankful to S. D. Mahanti for suggestions on improving the manuscript and to S. A. Trugman, R. Bhatt, T. A. Kaplan, V. Zelevinski, M. Mostovoy, I. Herbut, D. Mulhall, B. Nikolić and M. Milenković for inspiring discussions.

-
- [1] P. W. Anderson, Phys. Rev. **109**, 1492 (1958).
 - [2] D. J. Thouless, Phys. Lett. C **13**, 93 (1970).
 - [3] P. A. Lee and T. V. Ramakrishnan, Rev. Mod. Phys. **57**, 287 (1985).
 - [4] B. Kramer and A. MacKinnon, Rep. Prog. Phys. **56**, 1469 (1993).
 - [5] P. W. Anderson, D. J. Thouless, E. Abrahams, and D. S. Fisher, Phys. Rev. B **22**, 3519 (1980).
 - [6] D. C. Licciardello, D. J. Thouless, Phys. Rev. Lett. **35**, 1475 (1975).
 - [7] E. Abrahams, P. W. Anderson, D. C. Licciardello, and T. V. Ramakrishnan, Phys. Rev. B **42**, 673 (1979).
 - [8] A. MacKinnon and B. Kramer, Phys. Rev. Lett. **47**, 1546 (1981); Z. Phys. B **53**, 1 (1983).
 - [9] B. Huckestein, Rev. Mod. Phys. **67**, 357 (1995).
 - [10] G. Theodorou and M. Cohen, Phys. Rev. B **13**, 4597 (1976).
 - [11] L. Fleishman and D. C. Licciardello, J. Phys. C **10**, L125, (1977).
 - [12] C. M. Soukoulis and E. N. Economou, Phys. Rev. B **24**, 5698 (1981).
 - [13] F. Wegner, Phys. Rev. B **19**, 783 (1979).
 - [14] R. Gade, Nucl. Phys. B **398**, 499 (1993).

- [15] M. Inui, S. A. Trugman, and E. Abrahams, Phys. Rev. B **49**, 3190 (1994).
- [16] F. Wegner, Z. Phys. B **44**, 9 (1981).
- [17] Y. Hatsugai, X.-G. Wen, M. Kohmoto, Phys. Rev. B **56**, 1061 (1997).
- [18] Y. Morita and Y. Hatsugai, Phys. Rev. Lett. **79**, 3728 (1997); Phys. Rev. B **58**, 6680 (1998).
- [19] C. M. Soukoulis, I. Webman, G. S. Grest, and E. N. Economou, Phys. Rev. B **26**, 1838 (1982).
- [20] A. Eilmes, R. A. Römer, and M. Schreiber, Eur. Phys. J. B **1** 29, (1998).
- [21] J. Miler and J. Wang, Phys. Rev. Lett. **76**, 1461 (1996).
- [22] J. L. Pichard and G. Sarma, J. Phys. C **14**, L127 (1981); L617 (1981).
- [23] V. Z. Cerovski, S. D. Mahanti, T. A. Kaplan, and A. Taraphder, Phys. Rev. B **59**, 13977 (1999).
- [24] P. W. Brouwer, C. Mudry, and A. Furusaki, preprint No. cond-mat/9904201, (1999).
- [25] It is assumed here, without loss of generality, that $N_A \geq N_B$. The m zero-energy eigenstates still remain if arbitrary hoppings are introduced among sites of the sublattice B [15].
- [26] B. I. Shklovskii, B. Shapiro, B. R. Sears, P. Lambrianides, and H. B. Shore, Phys. Rev. B **47**, 11487 (1993).
- [27] D. Braun, G. Montambaux, and M. Pascaud, Phys. Rev. Lett. **81**, 1062 (1998).
- [28] I. Kh. Zarekeshev, M. Batsch, and B. Kramer, Europhys. Lett. **34**, 587 (1996).
- [29] F. Haake, *Quantum Signatures of Chaos* (Springer-Verlag, 1991). Unfolding by the cubic spline fitting was used.
- [30] Some preliminary results indicate that $D_1(s)$ has characteristics of the critical distribution, while other $D_i(s)$ have exponential tail characteristic for localized states.
- [31] H. Aoki, J. Phys. C **16**, L205 (1983); Phys. Rev. B **33**, 7310 (1986).
- [32] C. M. Soukoulis and E. N. Economou, Phys. Rev. Lett. **52**, 565 (1984).
- [33] V. I. Fal'ko, K. B. Efetov, Eur. Phys. Lett. **32**, 627 (1995); Phys. Rev. B **52**, 17413 (1995).
- [34] F. Wegner, Z. Phys. B **36**, 209 (1980).
- [35] C. Castellani and L. Peliti, J. Phys. A **19**, L429 (1986).
- [36] T. Hasley, M. Jensen, L. Kadanoff, I. Procaccia, and B. Shraiman, Phys. Rev. A **33**, 1141 (1986).
- [37] M. H. Jensen, L. P. Kadanoff, and I. Procaccia, Phys. Rev. A **36**, 1409 (1987).
- [38] $D_{q=1}$ is defined from the limit $q \rightarrow 1$ of the definition (15). See, *e.g.*, Ref. [9].
- [39] One may imagine that, in the spirit of the renormalization group analysis, weaker than power-law behavior should be possible as well. This indeed happens with two dimensional random Dirac fermions interacting with disordered non-Abelian vector potential, as shown in J.-S. Caux, N. Taniguchi, and A. M. Tsvelik, Phys. Rev. Lett. **80**, 1276 (1998).
- [40] S. N. Evangelou, Physica A **167**, 199 (1990).
- [41] J. Cardy, *Scaling and Renormalization in Statistical Physics*, (Cambridge University Press, 1996).
- [42] C. W. J. Beenakker, Rev. Mod. Phys. **69**, 731 (1997).
- [43] J. T. Chayes and L. Chayes, D. S. Fisher, and T. Spencer, Phys. Rev. Lett. **24**, 2999 (1986).

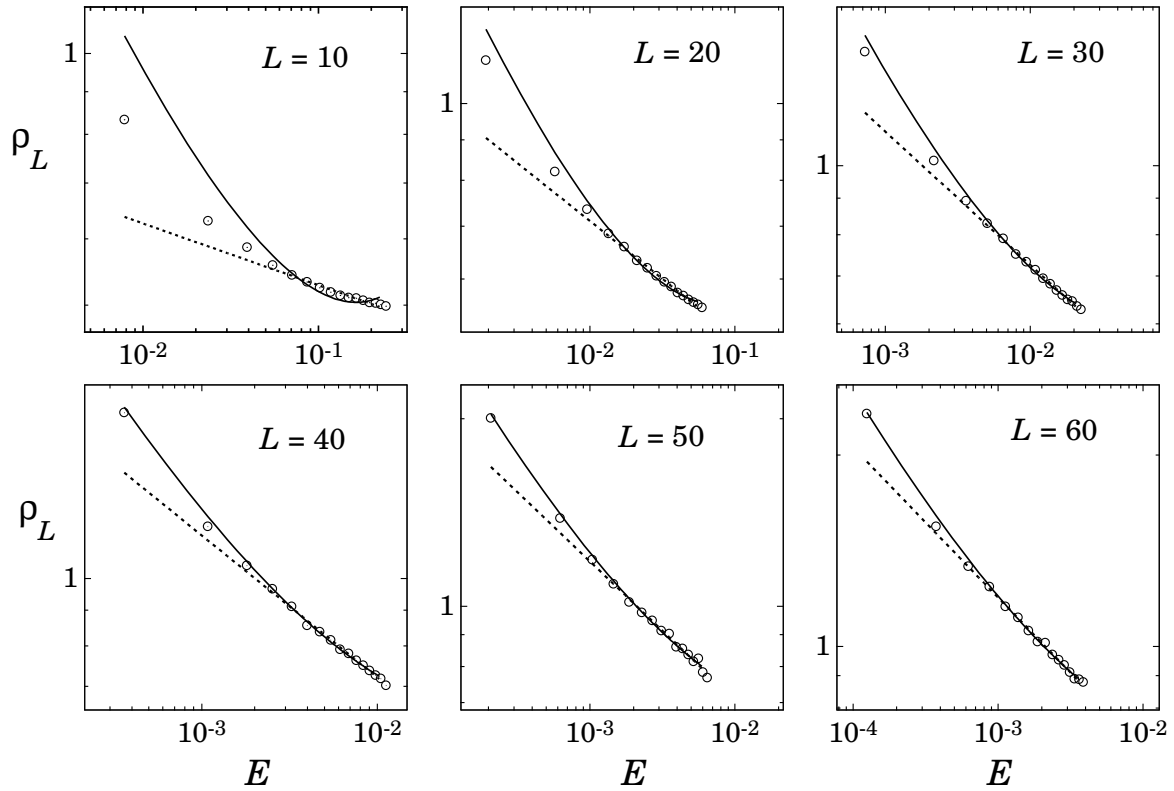


FIG. 1. Density of states $\rho_L(E)$ of the ABD model for $w = 1$ near the band center for system sizes $L = 10, \dots, 60$ in log-log plot. Full lines are fits to the Gade's form (6), while dotted lines are fits to the powerlaw. Fit to the Gade's form is done for all the points except the one closest to the band center, while fit to the powerlaw is done for all the bins except the three bins closest to the band center, which are the L -dependent parts of $\rho_L(E)$.

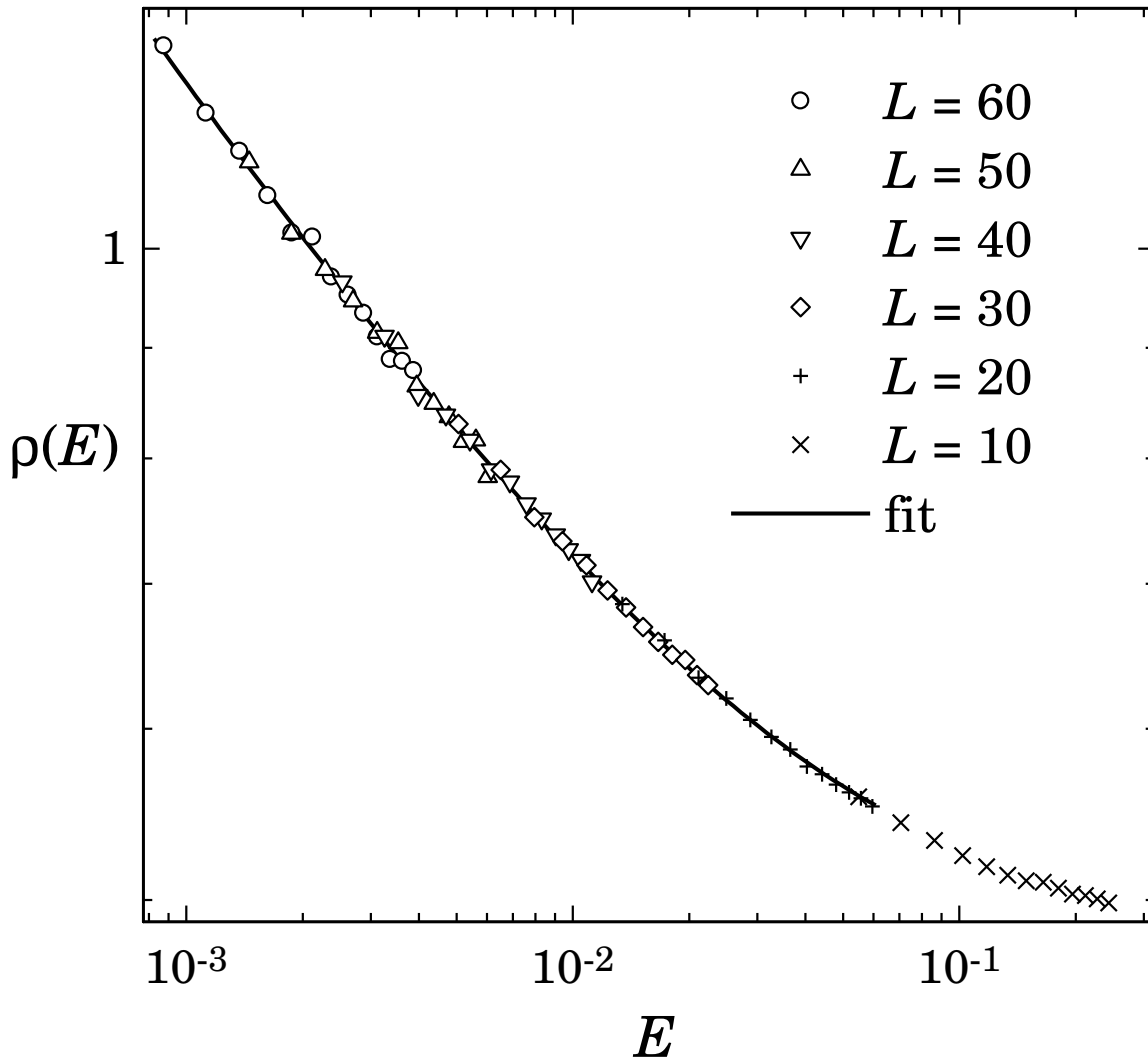


FIG. 2. Density of states of the ABD model for $w = 1$ near the band center. The graph is obtained from the data in Fig. 1 by removing the three bins closest to the band center, leaving the L -independent $\rho(E)$. The fit is $\rho(E) = C \exp(-\kappa\sqrt{-\ln|E|})/\sqrt{|E|}$, with $\kappa = 1.345 \pm 0.005$ and $C = 1.30 \pm 0.03$.

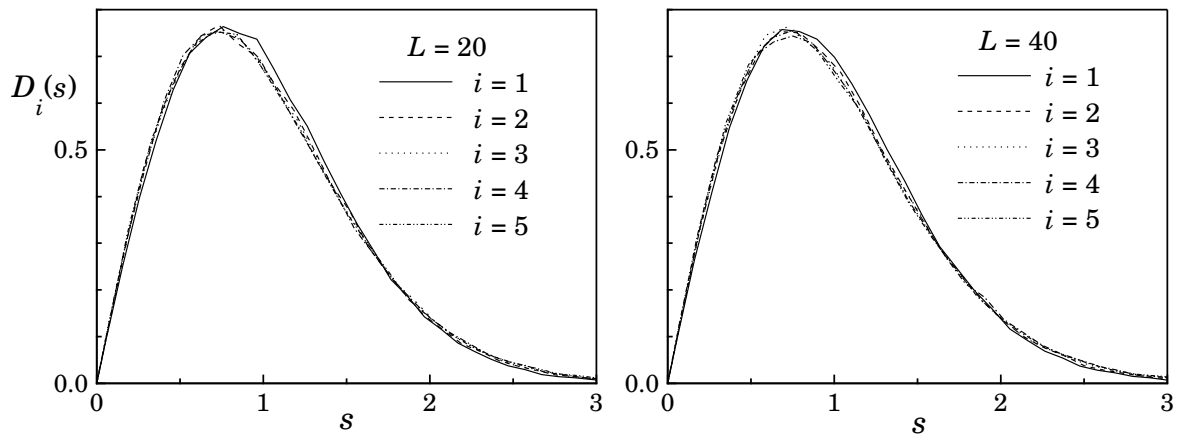


FIG. 3. Distributions of level spacings (after unfolding of the spectrum) $D_i(s)$ between i and $i + 1$ level, counted from the band center. $D_1(s)$ is distinctly different than other distributions due to the presence of the symmetry.

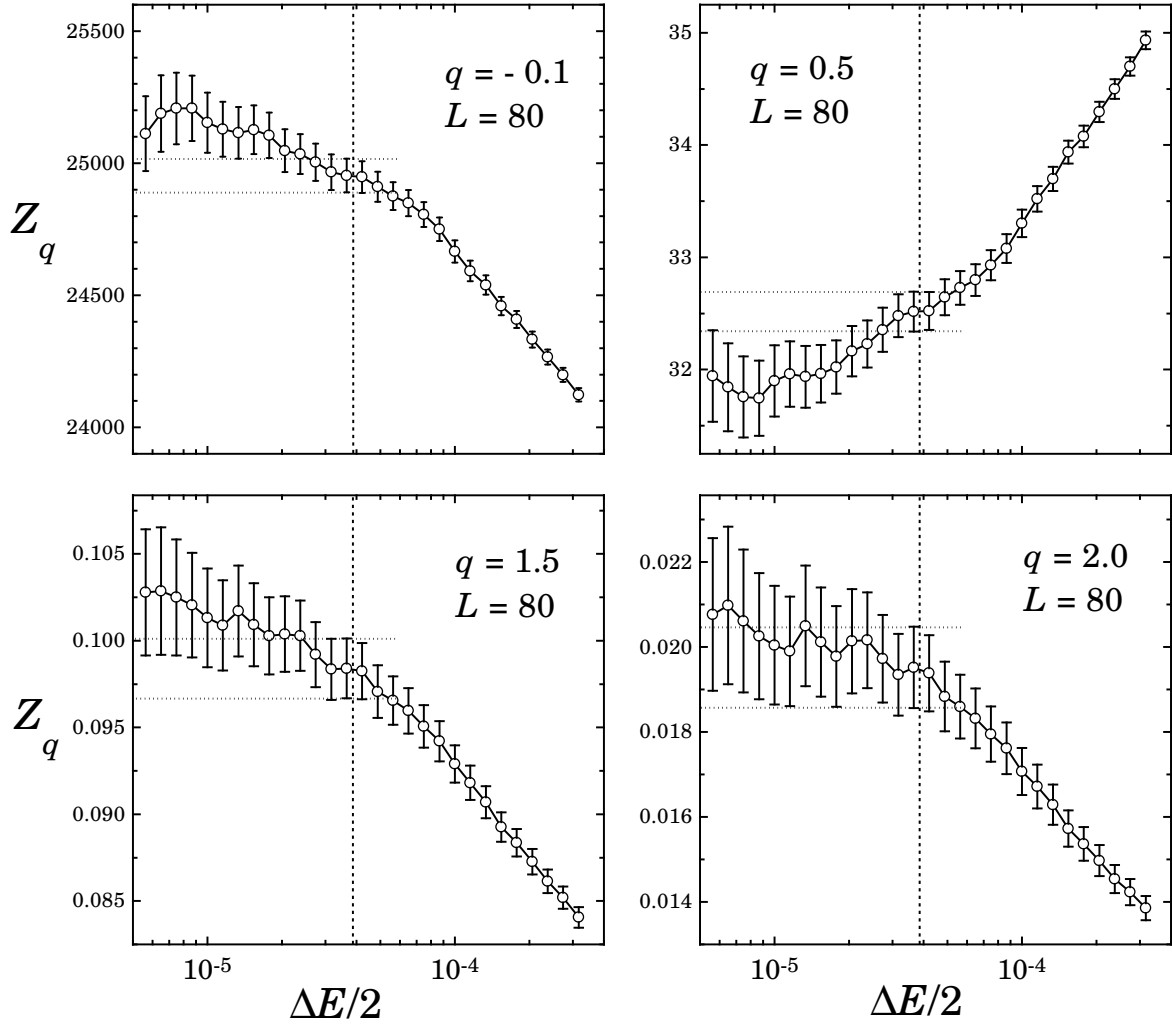


FIG. 4. Dependence of the average IPN for several different q 's and $L = 80$ on the bin size ΔE . The vertical dashed lines represent energies $E_2(L)/2$ (see text for discussion).

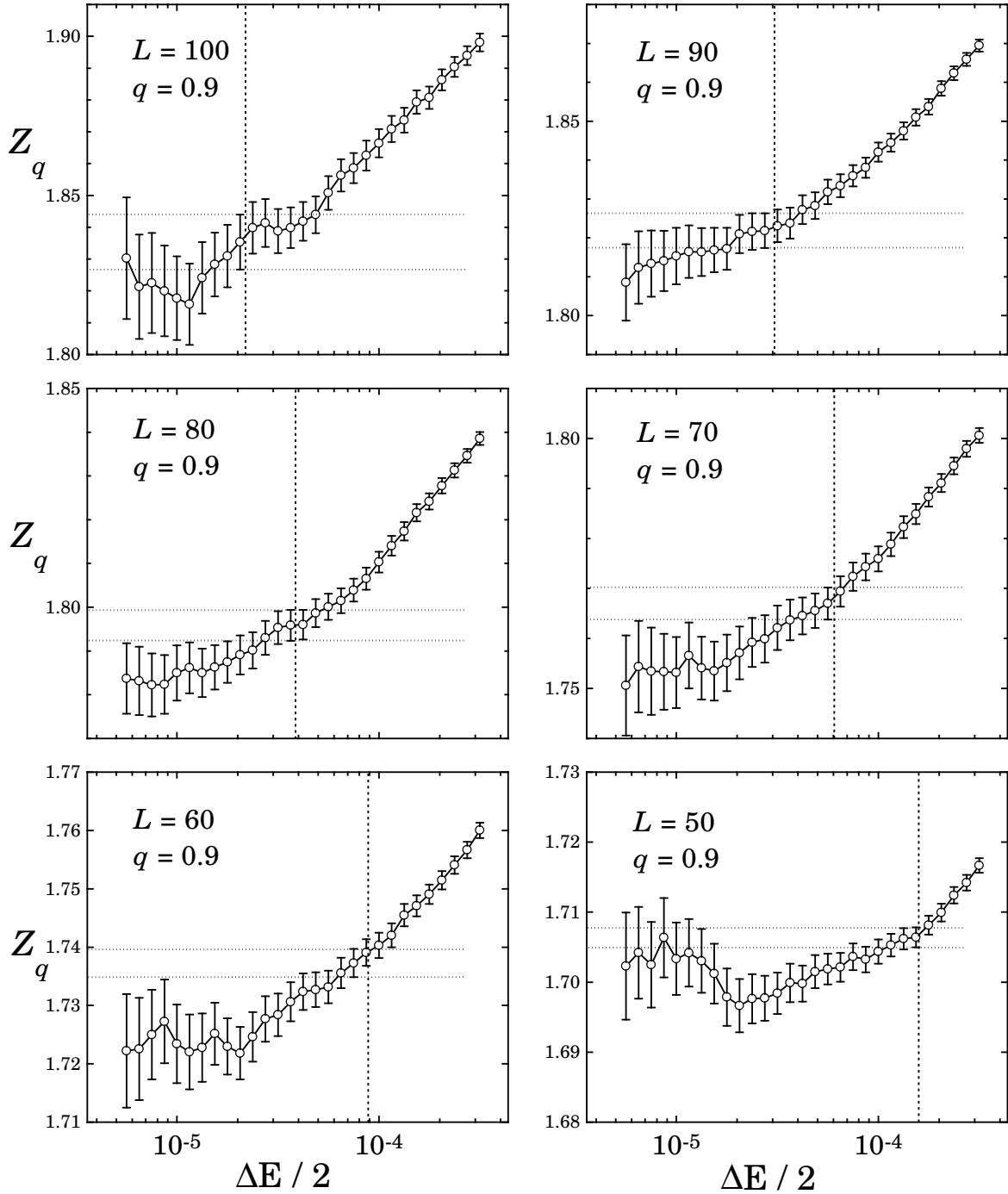


FIG. 5. Dependence of the average IPN for several different L and $q = 0.9$ on the bin size ΔE . The vertical dashed lines represent energies $E_2(L)/2$ (see text for discussion).

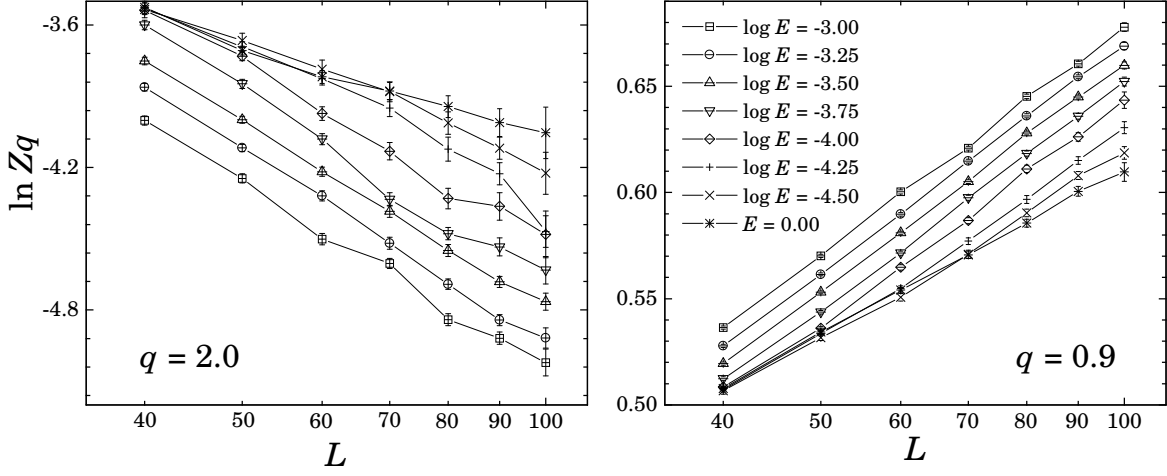


FIG. 6. Dependence of the average IPN on system size for several energies near the band center for $q = 0.9, 2$.

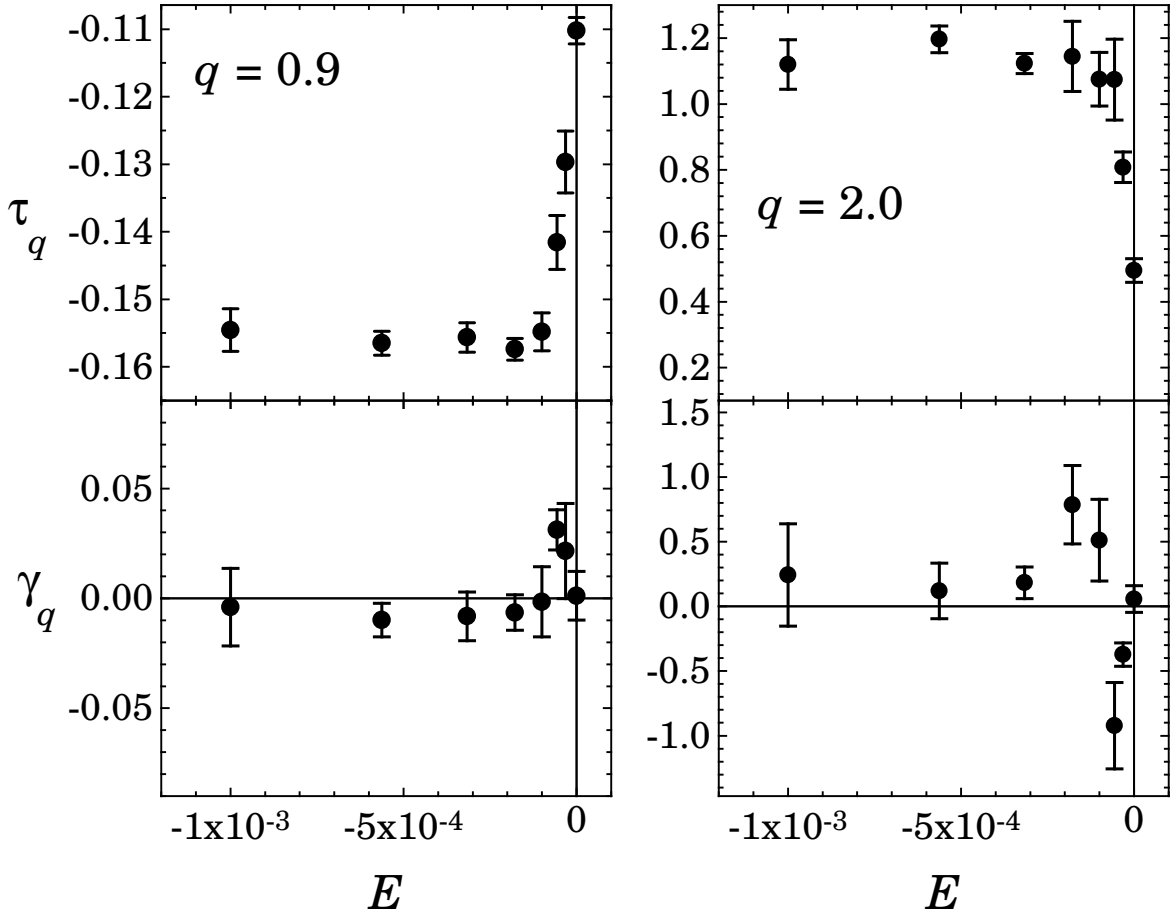


FIG. 7. Scaling exponent of IPN, τ_q , and the goodness of fit coefficient γ_q , calculated from the data in Fig. 6 (except $L = 40$ results).

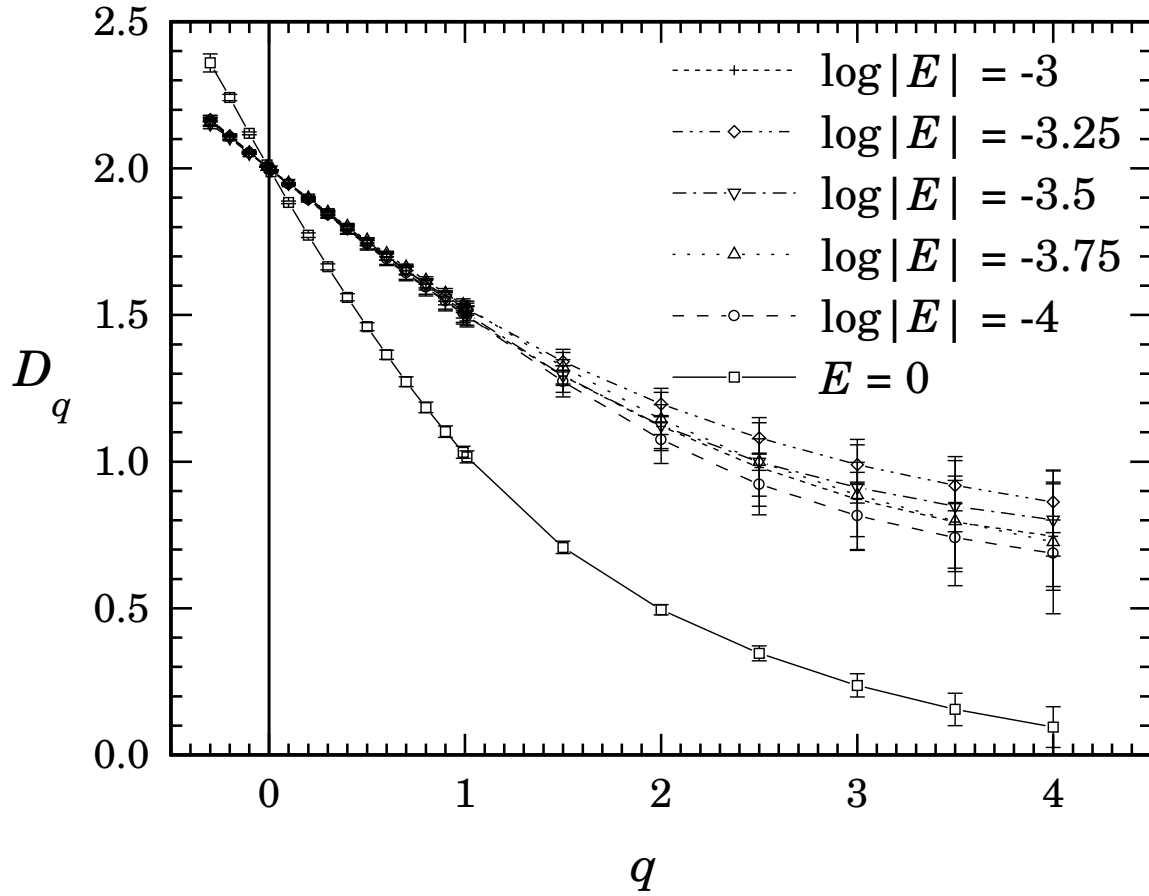


FIG. 8. Multifractal spectra D_q at the band center and nearby energies.

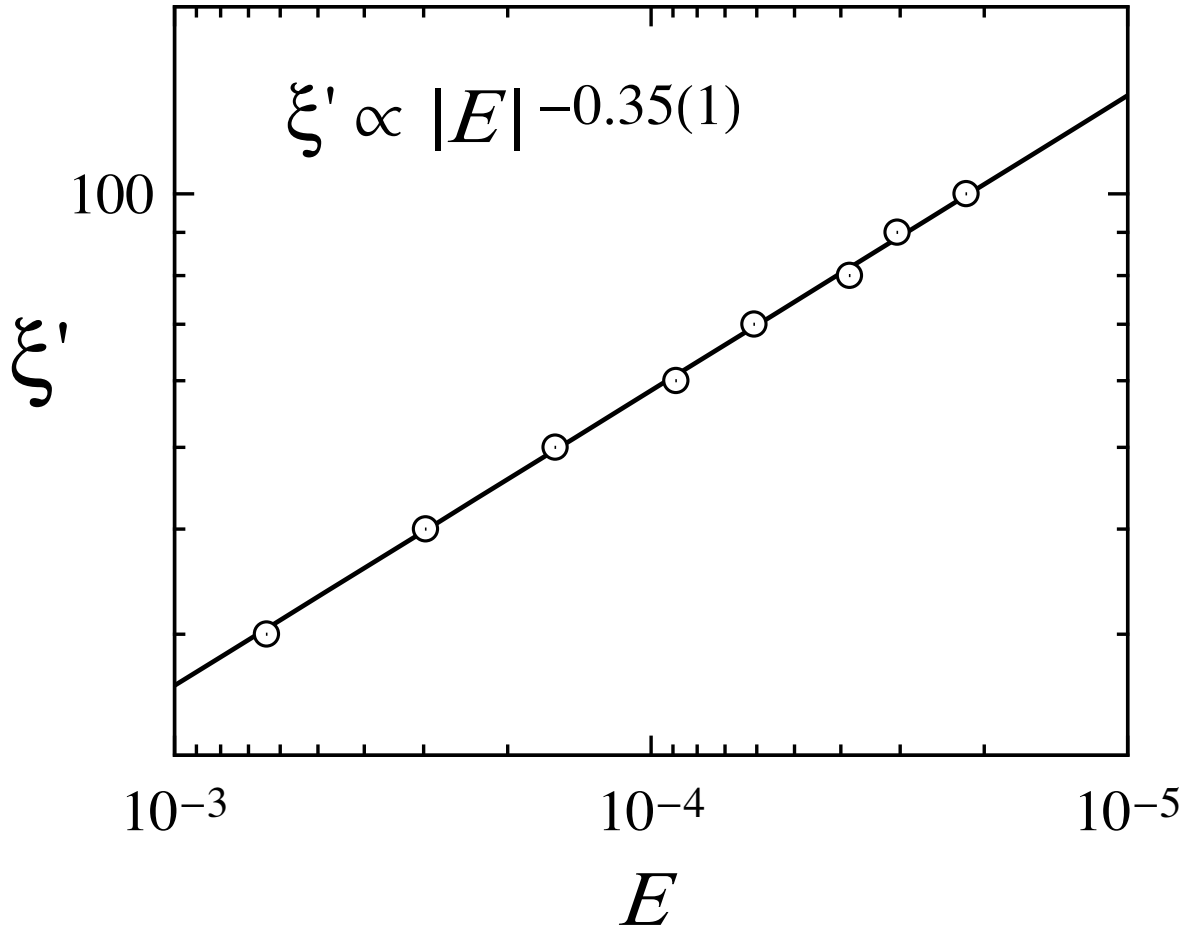


FIG. 9. Dependence of the new length scale on energy near the band center, as determined from the Eq. (17).

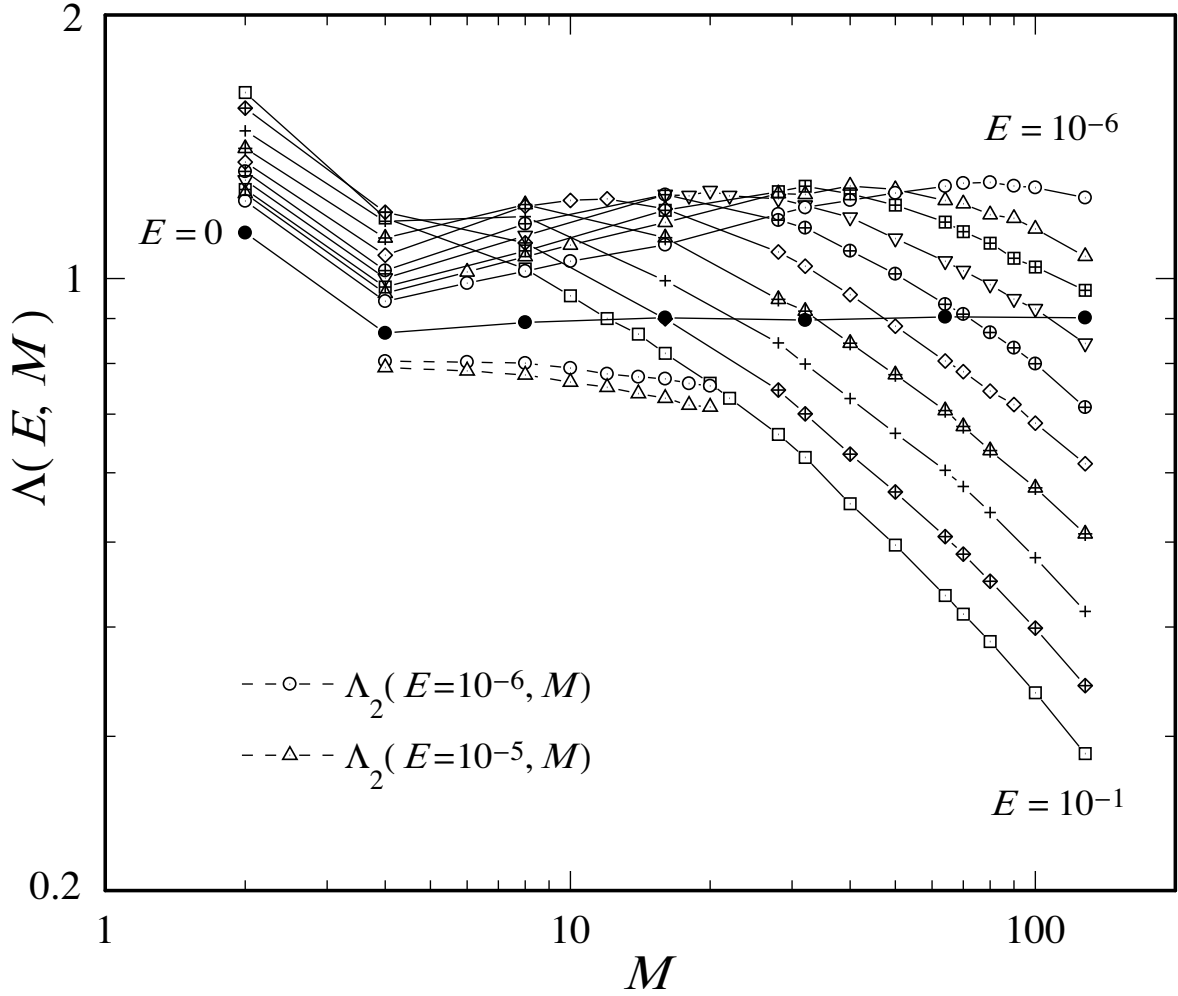


FIG. 10. The largest renormalized inverse Lyapunov exponents $\Lambda(E, M)$, calculated for long stripes of width M and various energies near the band center (full line). The energies range from $\log |E| = -1, -1.5, \dots, -5$, and additional $\log E = -6$. Dashed lines connect points of the second largest ILE, $\Lambda_2(E, M)$, for energies $E = 10^{-5}, 10^{-6}$, and $M \leq 20$.

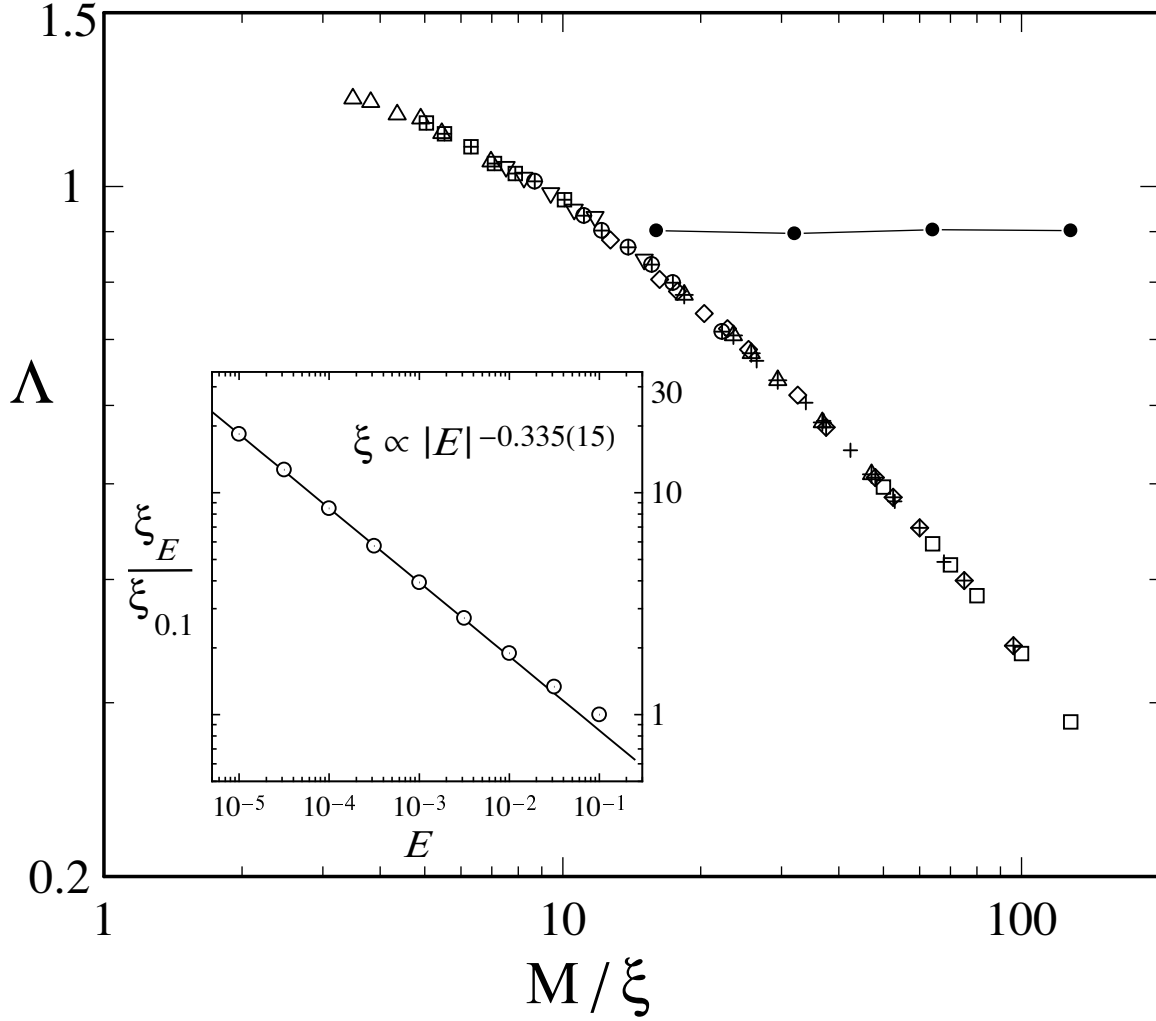


FIG. 11. One parameter universal function $\Lambda(M/\xi(E))$ for the ABD model. The four separate points are $\Lambda(E = 0, M)$ for $M = 16, 32, 64, 128$, corresponding to the band center critical state. The inset shows the calculated localization length $\xi(E)$ in units of the localization length $\xi(E = 0.1)$, with error bars smaller than the symbol size.